[Communication] doi: 10.3866/PKU.WHXB201602262 www.whxb.pku.edu.cn

硫基离子液体电解质拓宽量子点敏化太阳能电池的应用温度范围

史继富[1] 黄启章[1,2] 万青翠[1] 徐雪青[1,*] 李春生[3,*] 徐 刚[1,*]

([1]中国科学院广州能源研究所，中国科学院可再生能源与天然气水合物重点实验室，广东省新能源和可再生能源重点实验室，广州 510640；[2]中国科学院大学，北京 100049；[3]华北理工大学化工学院，河北 唐山 063009)

摘要：制备了1-甲基-3-丙基咪唑硫离子液体电解质，并应用在量子点敏化太阳能电池中。通过优化S和Na_2S的浓度，电解质的电导率在25 °C下达到了12.96 mS·cm^{-1}。差示扫描量热法分析表明离子液体电解质的玻璃化转变温度为−85 °C。采用该电解质的量子点敏化太阳能电池在25 °C下达到了3.03%的光电转化效率(η)，与采用水基电解质的电池的效率3.34%接近。由于本文中的离子液体电解质具有低玻璃化转变温度和不易挥发的优点，采用离子液体电解质的量子点敏化太阳能电池在−20 °C (η = 2.32%)及80 °C (η = 1.90%)的温度下表现出了比水基电解质优异的光电转化性能。

关键词：量子点敏化太阳能电池；离子液体电解质；1-甲基-3-丙基咪唑硫；应用温度；效率

中图分类号：O646

Sulfide-Based Ionic Liquid Electrolyte Widening the Application Temperature Range of Quantum-Dot-Sensitized Solar Cells

SHI Ji-Fu[1] HUANG Qi-Zhang[1,2] WAN Qing-Cui[1] XU Xue-Qing[1,*]
LI Chun-Sheng[3,*] XU Gang[1,*]

([1]*Guangzhou Institute of Energy Conversion, Key Laboratory of Renewable Energy and Gas Hydrate, Guangdong Key Laboratory of New and Renewable Energy Research and Development, Chinese Academy of Sciences, Guangzhou 510640, P. R. China*; [2]*University of Chinese Academy of Sciences, Beijing 100049, P. R. China*; [3]*College of Chemical Engineering, North China University of Science and Technology, Tangshan 063009, Hebei Province, P. R. China*)

Abstract: We report the preparation and application of a 1-methyl-3-propylimidazolium sulfide-based ionic liquid electrolyte for quantum-dot-sensitized solar cells. By optimizing the concentrations of S and Na_2S, a considerable conductivity of 12.96 mS·cm^{-1} is achieved at 25 °C. Differential scanning calorimetry indicates that the glass transition temperature of the electrolyte is −85 °C. The quantum-dot-sensitized solar cell assembled with this ionic liquid electrolyte displays a high energy conversion efficiency (η) of 3.03% at 25 °C, which is comparable to the efficiency of quantum-dot-sensitized solar cells using a water-based polysulfide electrolyte (η = 3.34%). Due to the favorable thermal properties of this ionic liquid electrolyte (lower glass transition temperature and nonvolatility at higher temperatures), the quantum-dot-sensitized solar cell maintains satisfactory η even at −20 °C (η = 2.32%) and 80 °C (η = 1.90%), which is superior to the cell using the water-

Received: January 22, 2016; Revised: February 25, 2016; Published on Web: February 26, 2016.

*Corresponding authors. XU Gang, Email: xugang@ms.giec.ac.cn. XU Xue-Qing, Email: xuxq@ms.giec.ac.cn; Tel: +86-20-87057592.
LI Chun-Sheng, Email: lichsheng@163.com.

The project was supported by the National Natural Science Foundation of China (21103194, 51506205), Science and Technology Planning Project of Guangdong Province, China (2014A010106018, 2013A011401011), Guangdong-Hong Kong Joint Innovation Project of Guangdong Province, China (2014B050505015), Special Support Program of Guangdong Province, China (2014TQ01N610), Director Innovation Foundation of Guangzhou Institute of Energy Conversion, China (y307p81001), and Solar Photothermal Advanced Materials Engineering Research Center Construction Project of Guangdong Province, China (2014B090904071).

国家自然科学基金(21103194, 51506205), 广东省科技计划(2014A010106018, 2013A011401011), 粤港合作项目(2014B050505015), 广东省特支计划(2014TQ01N610), 中国科学院广州能源研究所所长创新基金(y307p81001)及广东省太阳能光热先端材料工程技术研究中心建设项目(2014B090904071)资助

based polysulfide electrolyte.

Key Words: Quantum-dot-sensitized solar cell; Ionic liquid electrolyte; 1-Methyl-3-propylimidazolium sulfide; Application temperature; Efficiency

1 Introduction

Dye-sensitized solar cells (DSCs) with organic solvent-based electrolytes containing I_3^-/I^- redox couples and ruthenium complex dye have been intensively studied over the past decade and regarded as an alternative to the conventional inorganic device due to their high efficiency (η, ~13%) and low cost[1,2]. Recently, narrow-band gap inorganic quantum dots (QDs, such as CdSe, CdS, etc.) as next-generation sensitizers for DSCs have attracted more attention owing to their tunable band gaps[3], higher extinction coefficient[4,5]. Moreover, the solar cells sensitized by quantum dots (quantum-dot-sensitized solar cells, QDSCs) have the possibility of utilizing hot electrons to produce multiple electron-hole pairs per photon[6], and thus have a higher theoretical efficiency. For these QDSCs, the electrolyte plays an important role in the determination of the photovoltaic performance[7,8]. On one hand, it transfers the electrons to the oxidized QDs around the photoanode to make the QDs regeneration. On the other hand, the electrolyte accepts electrons around the photocathode to complete a cycle. At present, the most commonly used electrolyte in the QDSCs was the water-based polysulfide electrolyte[7,9], in which the polysulfide redox couples served as high efficient charge carriers. However, the temperature range of this water-based polysulfide electrolyte used is too narrow to meet the requirement of practical application[10]. When the temperature is lower, this water-based electrolyte will be freezed, which not only hinders the transport of the charge carriers in the electrolyte but also makes the interfacial contact between the electrolyte and porous TiO_2 film become poor. However, when the temperature is higher, this water-based electrolyte may suffer from volatilization, leading to ineffective link between photoanode and photocathode. Thus, the freeze and volatilization of the water-based electrolyte will lead to serious decrease of the η of the QDSCs. Using the organic solvent to replace the water is considered to be an alternative choice[11]. Nevertheless, the organic solvent will be also evaporated at high temperature and the solubility of S and Na_2S in organic solvent is too low to afford high photocurrent[11].

Ionic liquids (ILs) with 1,3-dialkylimidazolium cations and iodide anion have been successfully used in DSCs due to their favorable properties such as thermal stability, high ionic conductivity, and nonvolatility (negligible vapor pressure)[12,13]. For example, the DSCs with eutectic melts contained 1,3-dimethylimidazolium iodide, 1-ethyl-3-methylimidazolium iodide, 1-allyl-3-methylimidazolium iodide, and iodine yielded an η of 7.1% [13]. We also synthesized 1-ethyl-3-methylimidazolium isonicotinate electrolyte for DSCs with 4.3% efficiency recently[14]. However, these iodide-based IL electrolytes cannot be well applied to QDSCs because the presence of I_3^-/I^- redox couples will cause serious photocorrosion of QDs, which promotes us to explore the new ILs-based electrolyte to substitute the water-based electrolyte for the QDSCs. Thus, in this paper, we synthesized the 1-methyl-3-propylimidazolium sulfide (MPIS) IL, and applied this IL to QDSCs. This MPIS-based IL electrolyte can be used in a wide temperature range and shows a high η.

2 Experimental

2.1 Cell fabrication

2.1.1 MPIS-based IL electrolytes

All reagents used were of analytical grade. The preparation process of the MPIS-based IL electrolytes is shown in Fig.1. 1-Methyl- 3- propylimidazolium hydroxide (MPIOH) was first synthesized using anion exchange resin (201 × 7, supplied by the resin company of Nankai university) from 1-methyl-3-propylimidazolium bromide (Qianhui Company of Guangzhou)[14]. And then the MPIOH aqueous solution was reacted with hydrogen sulfide gas until pH = 12 to obtain the MPIS aqueous solution. The above MPIS solution was evaporated to dryness under reduced pressure at 70 °C and further dried in vacuum for 2 days at 80 °C. Characterization: ^{1}H NMR (600 MHz, DMSO): δ 0.84 (t, J = 7.4 Hz, 3H), 1.81 (m, J = 7.3 Hz, 2H), 3.90 (s, 3H), 4.17 (t, J = 7.11 Hz, 2H), 7.72 (d, J = 1.8 Hz, 1H), 7.77 (d, J = 1.8 Hz, 1H), 9.92 (s, 1H); ^{13}C NMR (150 MHz, DMSO): δ 138.75, 123.97, 122.21, 50.43, 35.98, 23.68, 10.67. Addition of the sulfur and Na_2S into the MPIS obtained the ILs electrolytes.

2.1.2 Photocathodes

The TiO_2 electrode configuration was a compact layer of TiO_2, a transparent layer (with thickness of 8 μm and average particle size of 20 nm, Degussa AG of Germany), and a scattering layer (with thickness of 4 μm and average particle size of 300−400 nm). These electrodes were sintered at 450 °C for 30 min. The mesoporous TiO_2 electrodes were *in situ* sensitized by CdSe QDs grown by successive ionic layer adsorption and reaction (SILAR)[9]. The Se^{2-} precursor solution (0.03 mol·L^{-1} Se^{2-} in ethanol) was first prepared according to the method developed by the group of Grätzel[15]. For CdSe growth, the electrodes were successively immersed in two different solutions for 1 min each: one consisting of 0.03 mol·L^{-1} $Cd(NO_3)_2$ dissolved in ethanol, another of 0.03 mol·L^{-1} Se^{2-} precursor ethanol solution. The above sensitization

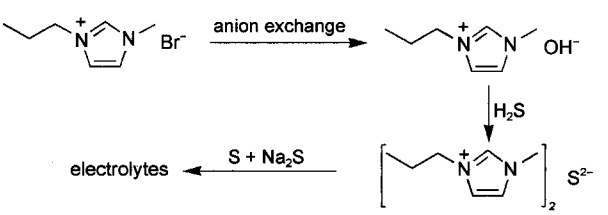

Fig.1 Preparation process of the MPIS-based IL electrolyte

process was carried out in the glovebox under N_2 atmosphere. After sensitization, the samples were further coated with ZnS by twice dipping alternately into 0.1 mol·L^{-1} $Zn(CH_3COO)_2$ and 0.1 mol·L^{-1} Na_2S solutions for 1 min/dip. The preparation of Cu_2S photocathodes was followed the optimal procedure of our previous report[16]. The Cu_2S photocathodes were prepared by immersing brass in HCl solution at 70 °C for 45 min and subsequently dropping water-based polysulfide electrolyte onto them for 10 s, resulting in porous Cu_2S electrodes. The water-based polysulfide electrolyte is composed of 1 mol·L^{-1} S, 1 mol·L^{-1} Na_2S, and 0.1 mol·L^{-1} NaOH in ultrapure water, which is a commonly used formula for electrolyte of QDSCs[9].

2.1.3 Assembling of QDSC

The QDSC was made by sandwiching the electrolyte between the prepared photoanode and photocathode. The two electrodes were separated by a Surlyn film hot-melt ring and sealed by heating. The photovoltaic measurements employed a class 3A solar simulator. The power of the simulated light was calibrated to be 100 mW·cm^{-2} by using a standard Si solar cell. The area of the cells was 0.21 cm^2.

2.2 Instruments and measurements

^{1}H and ^{13}C NMR spectra were carried out on Bruker AVANCE 600 MHz spectrometer (Bruker Company of Switzerland), using TMS as internal standard and DMSO as solvent. The thermograms were carried out with a NETZSCH DSC 204 analyzer (Netzsch Company of Germany) under N_2 atmosphere at a heating rate of 20 °C·min^{-1}.

The conductivity and its temperature dependence of the electrolyte were determined by impedance measurements PARSTAT 2273 Advanced Electrochemical System (Princeton Applied Research). The electrolyte was sandwiched between two mirror-finished stainless steel electrodes using a Teflon ring spacer in a constant volume cylindrical cell and was sealed with paraffin in the glove box. The sealed cell was maintained at various constant temperatures for at least 1 h prior to each measurement. The conductivity was calculated from the bulk resistance R_b. The cell constant was determined by calibration before and after measurement with 0.1 mol·L^{-1} KCl aqueous solution. Impedance experiments were performed on a computer-controlled Autolab Electrochemical System in the frequency range from 100 kHz to 100 mHz with an amplitude of 10 mV.

3 Result and discussion

3.1 Effect of composition on the conductivity of MPIS-based IL electrolyte

The MPIS-based IL electrolyte was optimized by adjusting the concentrations of S and Na_2S. First, the sulfur was added to MPIS to form the polysulfide redox couples. The relation between the sulfur concentration and the conductivity (σ) is shown in Fig.2(a). The ionic conductivity first increases and then decreases as the sulfur concentration increases, achieving the maximum value of 5.34 mS·cm^{-1} at the sulfur concentration of 1.5 mol·L^{-1}. The first increase of the conductivity is due to the formation of polysulfide chains, which makes the electrical conduction become easier. This

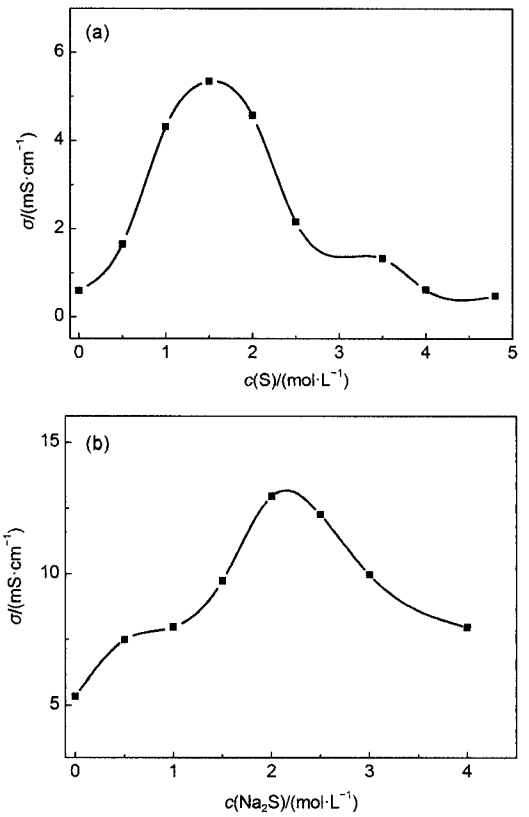

Fig.2 Influence of (a) S and (b) Na_2S concentrations on the conductivity of the MPIS-based IL electrolytes

phenomenon can be explained by a mechanism of electrical conduction in polysulfide chains *via* a Grotthus relay-type mechanism, where a net transport of charge is achieved by electron exchange reaction without any net transport of mass[17]. While, when the concentration of sulfur is beyond 1.5 mol·L^{-1}, the conductivity decreases probably because the surplus sulfur reduces the efficiency of carrier transferring[17]. So, the concentration of sulfur is fixed at 1.5 mol·L^{-1}.

In order to further improve the conductivity of the MPIS-based IL electrolyte system (with 1.5 mol·L^{-1} sulfur), Na_2S was added. The presence of Na_2S can increase the number of charge carriers. Fig.2(b) presents the variation of ionic conductivity as a function of the concentration of Na_2S. As expected, the conductivity is gradually improved as the Na_2S content increases. An exciting ionic conductivity of 12.96 mS·cm^{-1} is achieved at the Na_2S concentration of 2 mol·L^{-1}, which is about 2.4-fold higher than that without Na_2S. This value is also higher than the conductivity of pyrrolidinium sulfide ionic liquids electrolyte (5.34 mS·cm^{-1}), mainly attributing to the imidazolium cation that we employed with better conjugation for the alleviation of the electronstatic interaction between cations and anions as well as fluenter ion transport[18]. When the concentration of Na_2S is more than 2 mol·L^{-1}, the conductivity decreases, which may result from the aggregates or microcrystallites from excessive Na_2S blocking the transferring of carriers. The similar phenomenon was also observed in the polyiodide electrolyte system used in DSCs[17]. Thus,

the optimal electrolyte is composed of 1.5 mol·L^{-1} sulfur and 2 mol·L^{-1} Na_2S in MPIS.

3.2 Effect of temperature on the conductivity of the electrolytes

Fig.3(a) displays the temperature dependence of conductivity of the MPIS-based IL electrolyte. Even at −20 °C, the MPIS-based IL electrolyte still exhibits moderate conductivity of 1.46 mS·cm^{-1} and the conductivity increases with temperature because the transportation of charge carriers becomes faster at higher temperature. For example, the conductivity is up to 60.59 mS·cm^{-1} at 80 °C. The data in Fig.3(a) can be fitted well by Arrhenius equation (Eq.(1)):

$$\sigma(T) = A\exp\left[\frac{-E_a}{k_B T}\right] \quad (1)$$

where A is a constant, E_a is the activation energy, k_B is the Boltzmann constant, and T is the absolute temperature. The activation energy of the optimal MPIS-based IL electrolyte is calculated to be 27.46 kJ·mol^{-1}, which is similar to the values reported for IL system (20−54 kJ·mol^{-1})[19,20].

Surprisingly, for the water-based polysulfide electrolyte the increase of conductivity *versus* temperature doesn't display a simple linear relationship but two step temperature dependence (Fig.3(b)). In the first step (I, from 35 to 80 °C), the E_a is 6.95 kJ·mol^{-1}, and in the second step (II, from −20 to 30 °C), the E_a dramatically increases to 51.95 kJ·mol^{-1}, which is about 2-fold higher than that of MPIS-based IL electrolyte. Such a high value indicates inferior ionic conduction[21].

The different changing trend of the two electrolytes in Fig.3 can be explained by differential scanning calorimetry. Fig.4(a) is the thermogram of the optimal MPIS-based IL electrolyte. The glass transition temperature of this electrolyte is around −85 °C and no other phase transition signals can be observed with further increasing the temperature, as shown in Fig.4(a). That's why the data in Fig.2(a) can be fitted well by Arrhenius equation from −20 to 80 °C. This differential scanning calorimetry result also indicates the possibility that the optimal MPIS-based IL electrolyte can be used at lower temperature. Moreover IL has negligible vapor pressure, which can avoid the volatilization of electrolyte at higher

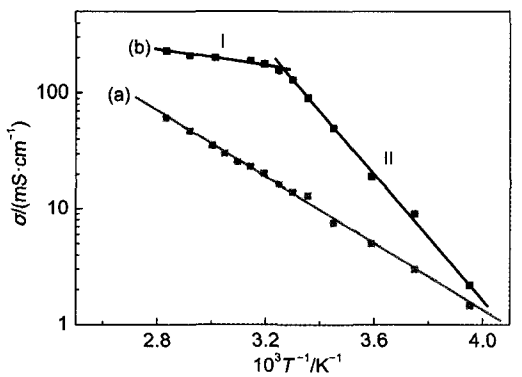

Fig.3 Temperature dependence of the conductivity of the (a) MPIS-based IL electrolyte and (b) water-based polysulfide electrolyte

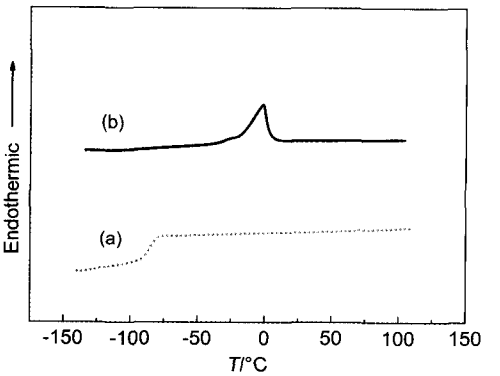

Fig.4 Differential scanning calorimetry thermograms of (a) MPIS-based IL electrolyte and (b) water-based polysulfide electrolyte

temperature. Thus, this MPIS-based IL electrolyte can be used in a wide temperature range. Fig.4(b) is the thermogram of water-based polysulfide electrolyte. The water-based polysulfide electrolyte displays a melting temperature (T_m) of −2 °C. When the temperature is lower than −2 °C, this water-based polysulfide electrolyte will be freezed, which will prevent the transport of the charge carriers in the electrolyte. In fact, the conductivity of this water-based polysulfide electrolyte begins to decrease rapidly when the temperature is lower than 30 °C as shown in Fig.2(b).

The photocurrent density−voltage curves for the cells with MPIS-based IL electrolyte (cell A) and water-based polysulfide electrolyte (cell B) are presented in Fig.5 and the data are summarized in Table 1. We have prepared 5 cells for each cell, and every cell is measured at least 2 times. The photocurrent density−voltage curves selected in this paper are the representative curves. For cell A measured at 25 °C, the open-circuit voltage (V_{oc}), short-circuit photocurrent density (J_{sc}), fill factor (FF) are 0.525 V, 17.9 mA·cm^{-2}, and 0.322, yielding a high η of 3.03%, which is comparable to the efficiency of QDSC with water-based polysulfide electrolyte (cell B, η = 3.34%) prepared and measured under the same condition (Fig.5 and Table 1). The slight lower efficiency of cell A has relation to the lower J_{sc} as shown in Fig.5 (a) and Table 1, which is mainly caused by the lower conductivity of the MPIS-based IL electrolyte compared with that of water-based polysulfide electrolyte.

As mentioned above, the MPIS-based IL electrolyte can be used in a wide temperature range due to its outstanding thermal properties. The photocurrent density−voltage curves of cell A and cell B measured at −20 and 80 °C are shown in Fig.5(b, c) and the data are also summarized in Table 1. For example, the conversion efficiency of cell A is 2.32% at −20 °C, which is higher than that of cell B (1.50%) at the same temperature. The lower η of cell B is mainly caused by the decreased J_{sc} (see Table 1). The freeze of water-based polysulfide electrolyte at this temperature hinders the transport of the charge carriers in the electrolyte and makes the interfacial contact between the electrolyte and porous TiO_2 film become poor, thus decreasing the J_{sc} of cell B.

When the temperature is increased, for example at 80 °C, the

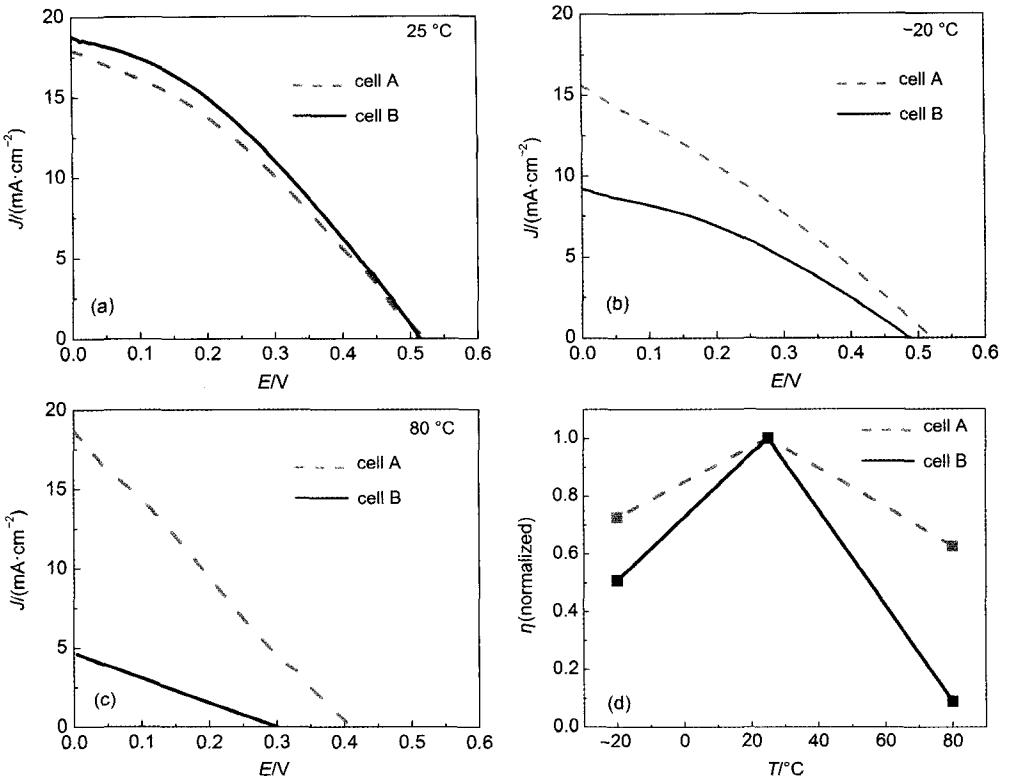

Fig.5 Comparison of photocurrent density–voltage curves (a–c) and η (d) of cell A and cell B at different temperatures

Table 1 Detailed photovoltaic performance parameters of V_{oc}, J_{sc}, FF, and η measured at different temperatures

Cell	T/°C	V_{oc}/V	J_{sc}/(mA·cm^{-2})	FF	η/%
A	−20	0.517	15.5	0.290	2.32
	25	0.525	17.9	0.322	3.03
	80	0.414	18.7	0.245	1.90
B	−20	0.489	9.2	0.334	1.50
	25	0.515	18.8	0.345	3.34
	80	0.301	4.59	0.251	0.347

V_{oc} of both cell A and cell B are obviously decreased due to the serious back reaction at higher temperature. However, the V_{oc} of cell A is still 113 mV higher than that of cell B probably because of the interaction between the 1-methyl-3-propylimidazolium cations and the TiO_2 film. This interaction perhaps has influence on the recombination, QDs regeneration, and electron transport in the titania film as observed in dye-sensitized solar cells[22]. The dark current curves in Fig.6 measured at 80 °C indicate MPIS-based IL electrolyte can inhibit the recombination between the electrons in TiO_2 film and the polysulfide ions in the electrolyte. We further measured the electrochemical impedance spectra (EIS) of cell A and cell B at 80 °C under moderate potential of −0.40 V (close to the V_{oc} of cell A)[23,24]. The calculated electron lifetime of cell A and cell B are 5.2×10^{-3} and 1.3×10^{-3} s, respectively. This result proves that the interaction between the 1-methyl-3-propylimidazolium cations and the TiO_2 film can restrain the recombination[25], which is in accordance with the dark current results in Fig.6. At 80 °C, the J_{sc} of cell B is decreased to 4.59 mA·cm^{-2} mainly

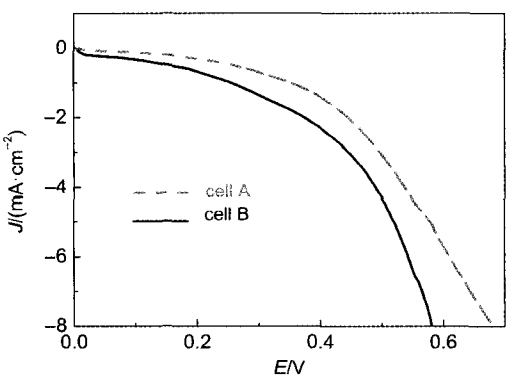

Fig.6 Dark current density curves of cell A and cell B measured at 80 °C

because of the volatilization of water. The volatilization of water leads to the ineffective link between photoanode and photocathode, thus limiting the transport of polysulfide ions in the cell. As a result, the η of cell B is sharply reduced to 0.347%. On the contrary, the MPIS-based IL electrolyte is non-volatile and its conductivity is increased at higher temperature. The above two factors together lead to an improved J_{sc} of cell A (J_{sc} = 18.7 mA·cm^{-2}), making cell A maintain a satisfactory η of 1.90% even at 80 °C. Fig.5(d) shows the normalized η of the two cells measured at different temperatures.

4 Conclusions

In summary, sulfur-based ionic liquid 1-methyl-3-propylimidazolium sulfide is prepared and applied in the QDSC for the first

time. By optimizing the contents of S and Na_2S, considerable conductivity of 12.96 $mS \cdot cm^{-1}$ is achieved. This optimal MPIS-based IL electrolyte has outstanding thermal properties of low glass transition temperature and nonvolatility, which make it can be used in a wide temperature range. The QDSC assembled with this MPIS-based IL electrolyte displays a high η of 3.03% at 25 °C, which is comparable to the efficiency of QDSC with water-based polysulfide electrolyte (η = 3.34%). Due to the favorable thermal properties of this MPIS-based IL electrolyte, the QDSC can maintain satisfactory η value even at −20 and 80 °C, which is obviously superior to the cell with water-based polysulfide electrolyte. This type of IL electrolyte is beneficial to promote the practical application of QDSCs.

References

(1) Mathew, S.; Yella, A.; Gao, P.; Humphry-Baker, R.; Curchod, B. F.; Ashari-Astani, N.; Tavernelli, I.; Rothlisberger, U.; Nazeeruddin, M. K.; Grätzel, M. *Nat. Chem.* **2014,** *6* (3), 242. doi: 10.1038/nchem.1861

(2) Moia, D.; Leijtens, T.; Noel, N.; Snaith, H. J.; Nelson, J.; Barnes, P. R. F. *Adv. Mater.* **2015,** *27* (39), 5889. doi: 10.1002/adma. 201501919

(3) Tian, J.; Lv, L.; Fei, C.; Wang, Y.; Liu, X.; Cao, G. *J. Mater. Chem. A* **2014,** *2* (46), 19653. doi: 10.1039/C4TA04534C

(4) Wang, S. M.; Dong, W. W.; Fang, X. D.; Deng, Z. H.; Shao, J. Z.; Hu, L. H.; Zhu, J. *Acta Phys. -Chim. Sin.* **2014,** *30* (5), 873. [王时茂, 董伟伟, 方晓东, 邓赞红, 邵景珍, 胡林华, 朱 俊. 物理化学学报, **2014,** *30* (5), 873.] doi: 10.3866/PKU.WHXB201403042

(5) Du, J.; Meng, X.; Zhao, K.; Li, Y.; Zhong, X. *J. Mater. Chem. A* **2015,** *3* (33), 17091. doi: 10.1039/C5TA04758G

(6) Bai, S. L.; Lu, W. H.; Li, D. Q.; Li, X. N.; Fang, Y. Y.; Lin, Y. *Acta Phys. -Chim. Sin.* **2014,** *30* (6), 1107. [白守礼, 陆文虎, 李殿卿, 李晓宁, 方艳艳, 林 原. 物理化学学报, **2014,** *30* (6), 1107.] doi: 10.3866/PKU.WHXB201404111

(7) Wei, H. Y.; Wang, G. S.; Wu, H. J.; Luo, Y. H.; Li, D. M.; Meng, Q. B. *Acta Phys. -Chim. Sin.* **2016,** *32* (1), 201. [卫会云, 王国帅, 吴会觉, 罗艳红, 李冬梅, 孟庆波. 物理化学学报, **2016,** *32* (1), 201.] doi: 10.3866/PKU.WHXB201512031

(8) Feng, W. L.; Li, Y.; Du, J.; Wang, W.; Zhong, X. H. *J. Mater. Chem. A* **2016,** *4* (4), 1461−1468. doi: 10.1039/C5TA08209A

(9) Sung, S. D.; Lim, I.; Kang, P.; Lee, C.; Lee, W. I. *Chem. Commun.* **2013,** *49* (54), 6054. doi: 10.1039/c3cc40754c

(10) Wang, Q. Y.; Chen, C.; Liu, W.; Gao, S. M.; Yang, X. C. *J. Nanopart. Res.* **2016,** *18* (1). doi: 10.1007/s11051-015-3314-9

(11) Lee, Y. L.; Chang, C. H. *J. Power Sources* **2008,** *185* (1), 584. doi: 10.1016/j.jpowsour.2008.07.014

(12) Wang, P.; Zakeeruddin, S. M.; Moser, J. E.; Nazeeruddin, M. K.; Sekiguchi, T.; Grätzel, M. *Nat. Mat.* **2003,** *2* (6), 402. doi: 10.1038/nmat904

(13) Bai, Y.; Cao, Y.; Zhang, J.; Wang, M.; Li, R.; Wang, P.; Zakeeruddin, S. M.; Grätzel, M. *Nat. Mat.* **2008,** *7* (8), 626. doi: 10.1038/nmat2224

(14) Wang, H.; Xu, X. Q.; Shi, J. F.; Xu, G. *Acta Phys. -Chim. Sin.* **2013,** *29* (3), 525. [王 海, 徐雪青, 史继富, 徐 刚. 物理化学学报, **2013,** *29* (3), 525.] doi: 10.3866/PKU.WHXB201301091

(15) Lee, H.; Wang, M.; Chen, P.; Gamelin, D. R.; Zakeeruddin, S. M.; Grätzel, M.; Nazeeruddin, M. K. *Nano Lett.* **2009,** *9* (12), 4221. doi: 10.1021/nl902438d

(16) Shi, J. F.; Fan, Y.; Xu, X. Q.; Xu, G.; Chen, L. H. *Acta Phys. -Chim. Sin.* **2012,** *28* (4), 857. [史继富, 樊 烨, 徐雪青, 徐 刚, 陈丽华. 物理化学学报, **2012,** *28* (4), 857.] doi: 10.3866/PKU.WHXB201202204

(17) Wu, J.; Hao, S.; Lan, Z.; Lin, J.; Huang, M.; Huang, Y.; Li, P.; Yin, S.; Sato, T. *J. Am. Chem. Soc.* **2008,** *130* (35), 11568. doi: 10.1021/ja802158q

(18) Jovanovski, V.; González-Pedro, V.; Giménez, S.; Azaceta, E.; Cabañero, G. N.; Grande, H.; Tena-Zaera, R.; Mora-Seró, I. N.; Bisquert, J. *J. Am. Chem. Soc.* **2011,** *133* (50), 20156. doi: 10.1021/ja2096865

(19) Abbott, A. P.; Boothby, D.; Capper, G.; Davies, D. L.; Rasheed, R. K. *J. Am. Chem. Soc.* **2004,** *126* (29), 9142. doi: 10.1021/ja048266j

(20) Zhou, Z. B.; Matsumoto, H.; Tatsumi, K. *ChemPhysChem* **2005,** *6* (7), 1324. doi: 10.1002/cphc.200500094

(21) Shi, J.; Chen, J.; Li, Y.; Zhu, Y.; Xu, G.; Xu, J. *J. Power Sources* **2015,** *282*, 51. doi: 10.1016/j.jpowsour.2015.02.022

(22) Hagfeldt, A.; Boschloo, G.; Sun, L.; Kloo, L.; Pettersson, H. *Chem. Rev.* **2010,** *110* (11), 6595. doi: 10.1021/cr900356p

(23) Huo, Z. P.; Tao, L.; Wang, S. M.; Wei, J. F.; Zhu, J.; Dong, W. W.; Liu, F.; Chen, S. H.; Zhang, B.; Dai, S. Y. *J. Power Sources* **2015,** *284*, 582. doi: 10.1016/j.jpowsour.2015.03.049

(24) Farooq, W. A.; Fatehmulla, A.; Aslam, M.; Atif, M.; Ali, S. M.; Yakuphanoglu, F.; Yahia, I. S. *J. Nanoelectron. Optoe.* **2014,** *9* (5), 671. doi: 10.1166/jno.2014.1653

(25) Chen, J.; Lei, W.; Deng, W. Q. *Nanoscale* **2011,** *3* (2), 674. doi: 10.1039/C0NR00591F